

# EFFECT OF HIGH HDROSTATIC STRESS ON THE FATIGUE BEHAVIOUR OF METALLIC MATERIALS

*I.Koutiri<sup>1</sup>, F.Morel.<sup>1</sup>, D.Bellett<sup>1</sup>, L.Augustins<sup>2</sup>*

<sup>1</sup>*Arts et métiers ParisTech, Laboratoire Procédés Matériaux Instrumentation  
Centre Angers, 49 035, Angers Cedex;*

<sup>2</sup>*P.S.A. Peugeot Citroën - Direction de la Recherche pour l'Innovation  
Automobile Mécanique Appliquée des Solides et Structures, Route de Gisy, 78943  
Vélizy Villacoublay*

Abstract: This work deals with the effect of high mean stress on the high cycle fatigue behavior of a cast aluminum alloy AlSi7Cu0.5Mg0.3. Uniaxial fatigue tests have been carried out at different load ratios, ranging from  $R=-1$  (push-pull) to  $R=0.95$ . In addition, in-situ meso-scale observations, using a optical microscope have also been performed during the tests. The aim of these observations is to identify the different crack initiation mechanisms that occur at different mean stress values. These mechanisms are directly related to the material microstructure and the evolutions of plastic deformation and material damage as a function of the imposed loading condition. Specimen fracture surfaces were consequently examined using a scanning electronic microscope (SEM). Two different fatigue crack mechanisms are clearly identified. These observations will be used to establish a fatigue criterion capable of taking into account the change in mechanism and therefore be applicable to the complete range of mean stress values.

## 1 INTRODUCTION

The ongoing quest for greater performance at a lower cost in the transport and other mechanical industries results in components being used under increasingly severe service conditions. This is the case in the design of diesel engine cylinder heads and can lead to the occurrence of fatigue problems. The cyclic stress state found in these cast aluminum components can be classed, in terms of fatigue, as an “extreme” condition. That is, the stress amplitudes (due to internal combustion) are typically very small but the mean or static stresses are very high (due to tightening, thermal effects, and residual stresses introduced via the manufacturing process). In addition the stress state is typically highly multiaxial. These “extreme” loading conditions create difficulties when sizing these components, firstly because it has been shown that classical multiaxial fatigue criteria are inappropriate in this fatigue regime [1] and secondly because very little fatigue data for these loading conditions exists in the literature (for very few materials). This data is fundamental for the identification and validation of fatigue models.

The purpose of this work is to understand the effect of a mean stress, and specifically VERY high mean stress, on the fatigue behavior of the cast aluminum

material used by PSA - Peugeot Citroën to fabricate their cylinder heads and to test the multiaxial fatigue criterion currently used by PSA (i.e. the Dang Van criterion). Note that the work presented in this article is limited to the study of uniaxial, tensile/bending loading conditions. Also, for reasons of confidentiality, no absolute values for the fatigue data are given in the article.

## 2 MATERIAL

The material studied in this work is the hypoeutectic cast aluminum alloy AlSi7Cu0.5Mg0.3. Its chemical composition is given in Table I.

Table 1 - Chemical composition (% weight)

	Fe	Si	Cu	Mg	Zn
Min (%)	-	6,50	0,40	0,28	-
Max(%)	0,20	7,50	0,60	0,35	0,10
	Mn	Ni	Ti	Pb	Sn
Min (%)	-	-	0,08	-	-
Max(%)	0,10	0,05	0,20	0,05	0,05

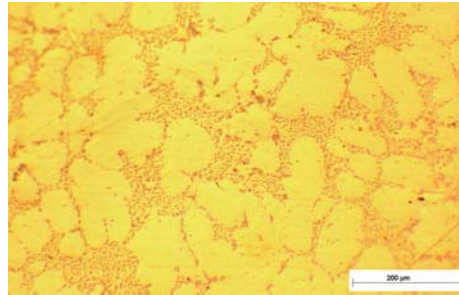


Figure 1 - Microstructure of AlSi7Cu0.5Mg0.3

The microstructure (see Figure 1) consists of aluminium ( $\alpha$  phase) dendrites surrounded by eutectic silicon particles. Prior to casting, refinement of the size of the  $\alpha$  phase dendrites is done via the addition of titanium and boron to the metal liquid, the silicon particles are modified via the addition of strontium and the liquid metal is degassed via the injection of nitrogen.

After casting, the material is solution heat treated for 4h at 535°C, water quenched at 70°C and then tempered at 200°C for 5 hours.

This treatment results in the following mechanical properties:

0.2% Offset Yield Strength, $\sigma_y$	Ultimate Tensile Strength, $\sigma_{UTS}$	Percent elongation at break, A
250 MPa	318 MPa	2 %

An important characteristic of this material is the presence of micro-shrinkage pores caused primarily by the volume contraction accompanying solidification. It is well known that these “defects” have a large influence on the fatigue strength of the material [2].

## 3 FATIGUE TESTS

Plane bending fatigue tests were performed on a resonant testing machine at a frequency of approximately 80 Hz. Smooth, rectangular shaped test specimens were machined directly from cylinder heads, cast by PSA, in order to characterize the real material and manufacturing process. The specimens were manually polished using carbon-silicon sand paper to a roughness of approximately Ra=0.2μm.

Four different load ratios were investigated:

- $R = -1$  (Zero mean stress,  $\sigma_m = 0 \text{ MPa}$ ),
- $R = 0.1$
- $R = 0.62$  (Maximum stress is slightly less than the yield stress,  $\sigma_{\max} \leq \sigma_y$ )
- $R = 0.95$  (Maximum stress is close to the ultimate stress, ( $\sigma_{\max} \approx \sigma_{UTS}$ )).

For each load ratio, the fatigue limit was evaluated using the staircase method, with 10 specimens, at  $2 \times 10^6$  cycles. For  $R = -1$  and  $R = 0.1$  a staircase with a fixed load ratio was used. For  $R = 0.62$  and  $R = 0.95$  a staircase with a fixed maximum stress was used.

As a resonance testing machine was used it was possible to use a change in frequency to define failure of the specimen. A decrease of 0.1Hz resulted in crack lengths of approximately 3 mm.

The results from these tests are summarized in Figure 2 in the form of a classical Haigh diagram. The well known Goodman and Gerber empirical criteria are also shown on this figure. It can be seen that, for the material discussed here, these criteria result in reasonably good prediction for the uniaxial mean stress effect.

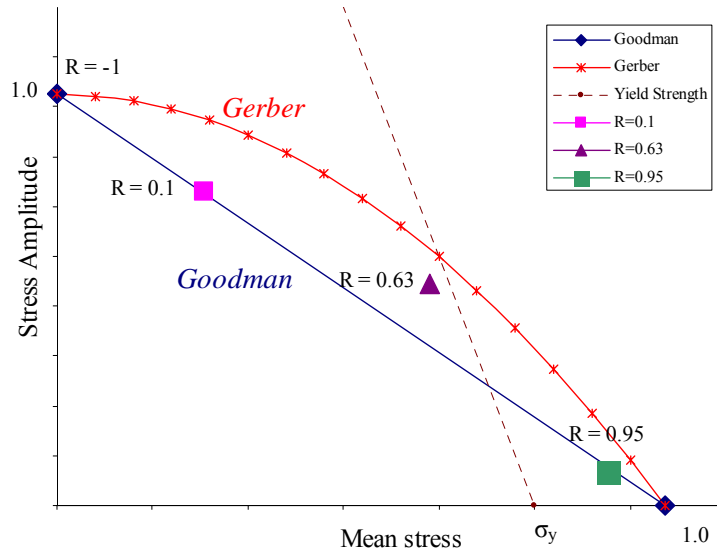


**Figure 2 - Haigh Diagram**

It should be noted that the fatigue limits represented on Figure 2 are for 50% probability of failure. Concerning the experimental scatter it was observed that the dispersion is lower when the mean stress high. The experimental scatter is approximately  $\pm 30 \text{ MPa}$  when  $R = -1$  and  $R = 0.1$ ;  $\pm 7 \text{ MPa}$  when  $R = -0.62$  and  $\pm 5 \text{ MPa}$  when  $R = 0.95$ .

## 4 IN-SITU OBSERVATIONS

In-situ mesoscopic observations using an optical microscope have been performed in order to observe the fatigue crack initiation mechanisms occurring at different load ratio. These observations were made on specimens loaded in uniaxial tension, using a servo-hydraulic Instron testing machine.

### 4.1 *In-situ observations at low mean stress ( $R=-1$ and $0.1$ )*

At low mean stress, fatigue crack initiation, in this material, is clearly controlled by micro-shrinkage pores. Figure 3b shows the SEM image of a typical defect of this type on the fracture surface of a specimen. Specifically, fatigue cracks initiate in the eutectic zone around a shrinkage pore due to the local stress concentration caused by the pore (see Figure 3a). The eutectic zones contain a high percentage of silicon particles, which are harder and more fragile than the aluminum dendrites. Consequently cracks form and propagate more easily in these zones. In addition, cracks tend to initiate at shrinkages pores located on or near the surface of the specimen. The distribution of the size of the micro-shrinkage pores has a strong influence on the fatigue strength of the material.

This crack initiation mechanism has been reported by other authors [3, 4].

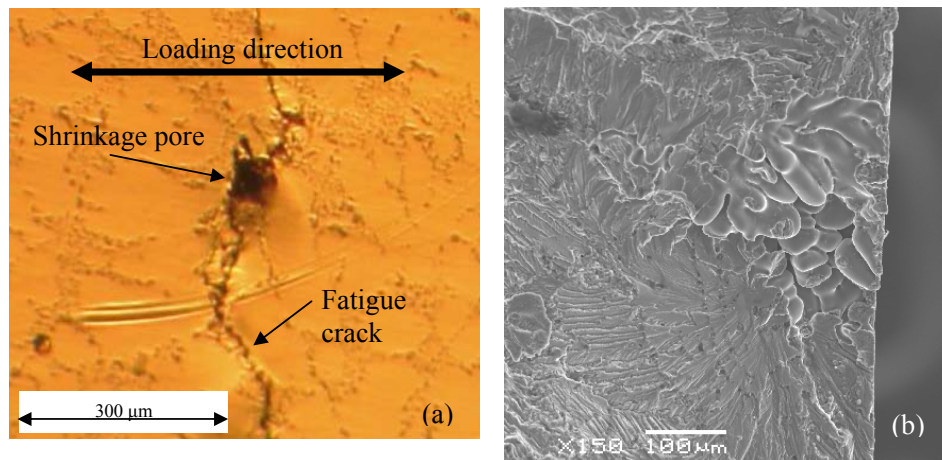


**Figure 3 – (a) Fatigue crack occurring at a pore and propagating along the eutectic zone; (b) SEM image of a fatigue rupture surface showing a micro-shrinkage pore**

### 4.2 *In-situ observations at high mean stress ( $R= 0.95$ )*

The first thing that must be noted, is that at the highest load ratio ( $R=0.95$ ) the maximum stress is very close to the ultimate tensile strength of the material and considerable greater than the yield stress (see Figure 2). As discussed below, this fact leads to a change in the high cycle fatigue crack initiation mechanism.

In this loading condition a large degree of “material damage” is created in the first  $\frac{1}{4}$  cycle (or the initial monotonic increase in load). This damage is clearly visible in Figure 4 and can be described as local rupture or decohesion of the material in

the eutectic zones containing a large number of silicon particles. This damage is not necessarily associated with micro-shrinkage pores. The average size of the damage is approximately 200  $\mu\text{m}$  and there is no preferred orientation with respect to the loading direction. However the damage is approximately uniformly distributed over the surface of the specimen.

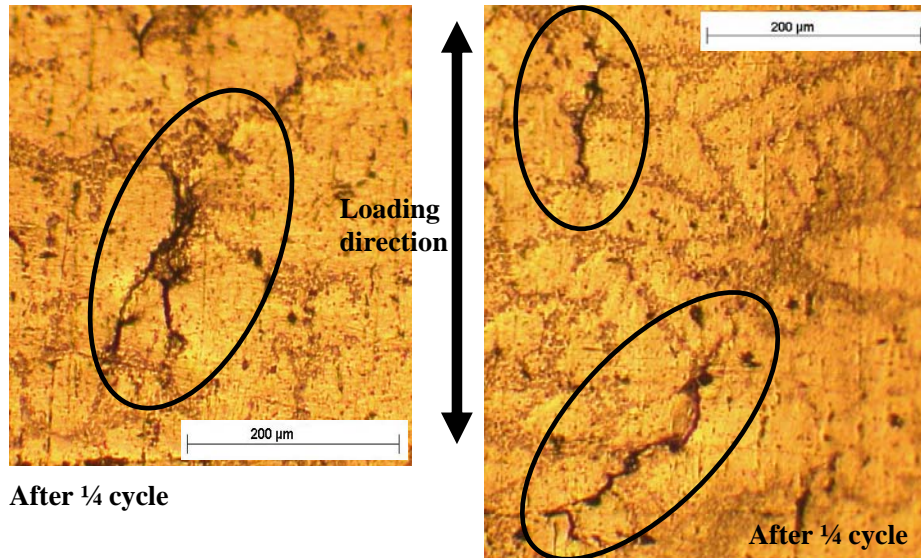


**Figure 4 - Appearance of “material damage” after a 1/4 cycle at R=0.95**

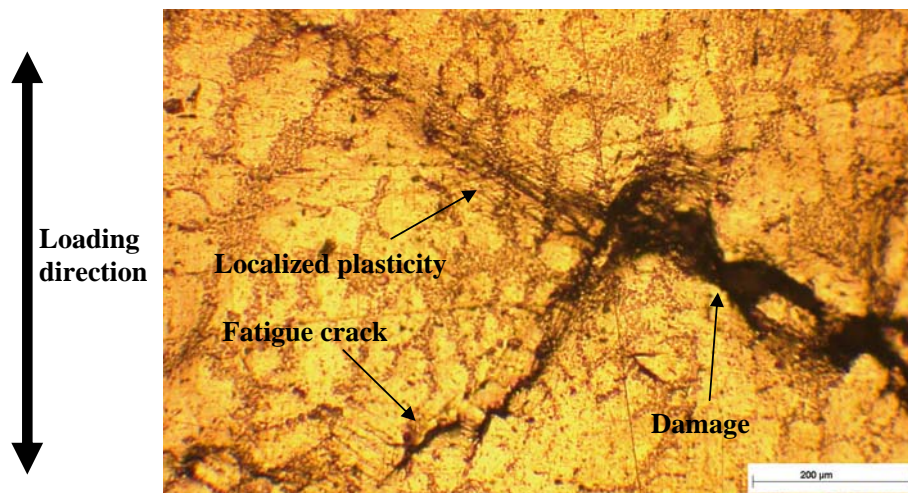


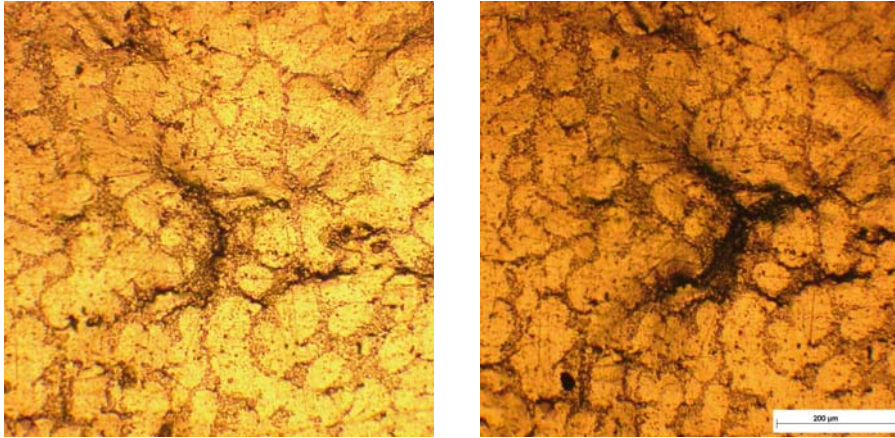
**Figure 5 –A zone showing *material damage* introduced in the first 1/4 cycle, *localised plasticity* occurring in slip planes and a *fatigue crack*, after 4000 cycles at R=0.95**

At this point it is important to define the terminology used in this article. The term “*material damage*” is used to describe the local rupture phenomenon previously discussed. The word “*crack*” is reserved to mean a high cycle fatigue crack in the

classical sense and “*localized plasticity*” is used to describe the permanent deformation occurring in slip planes, resulting in localized surface relief.

These three phenomena can be seen in Figure 5, which was taken after 4000 cycles at R=0.95. From this image it can be seen that both damage and crack propagation occur preferentially in the silicon rich eutectic zones of the material, while localized plasticity occurs in parallel bands generally at 45 degrees to the loading direction.

The next step was to try and observe the evolution of the damage/crack as a function of the number of cycles. Figure 6 shows the same damaged zone after 4000 and 15000 cycles. It can be seen that there is a very slight increase in the size of the damaged zone. No real increase in crack size is observed.



**(a) After 4000 cycles at R=0.95**

**(b) After 15000 cycles at R=0.95**

**Figure 6 – Change in the damage/crack size after cycling**

## 5 FAILURE SURFACE OBSERVATIONS AT R=0.95

Scanning Electron Microscope observations of the failure surfaces from the fatigue tests discussed above (at R=0.95) have also been undertaken. Figure 7 shows a SEM image of a typical fatigue failure surface. Figure 8 is a schematic representation of the key features seen.

From these figures, the fatigue mechanism operating at very high mean stress is clear. Three distinct zones can be observed:

- Zone I – is due to *material damage* primarily created in the first  $\frac{1}{4}$  cycle. For the specimen shown in Figure 7, this zone is centered on a sub-surface micro-shrinkage pore. This damage is due to ductile rupture as ductile dimples can be seen (in the zoomed image) of the fracture surface in this zone.
- Zone II – is a typical fatigue crack propagation failure surface for this material.
- Zone III – is due to unstable crack propagation when the fatigue crack reaches a critical size.

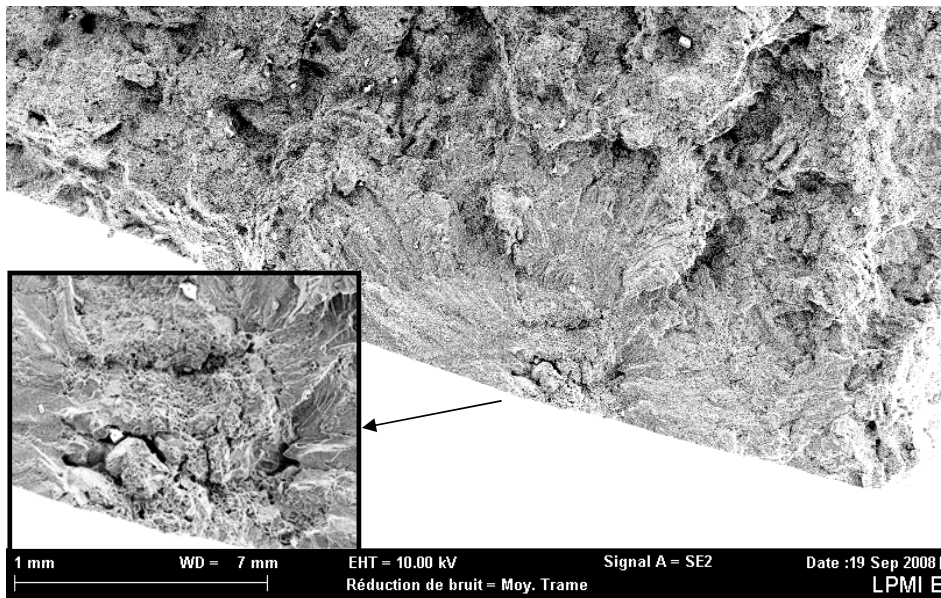


**Figure 7 – SEM image of a typical fatigue failure surface at R=0.95 (number of cycles to failure is  $5.5 \times 10^5$  cycles)**

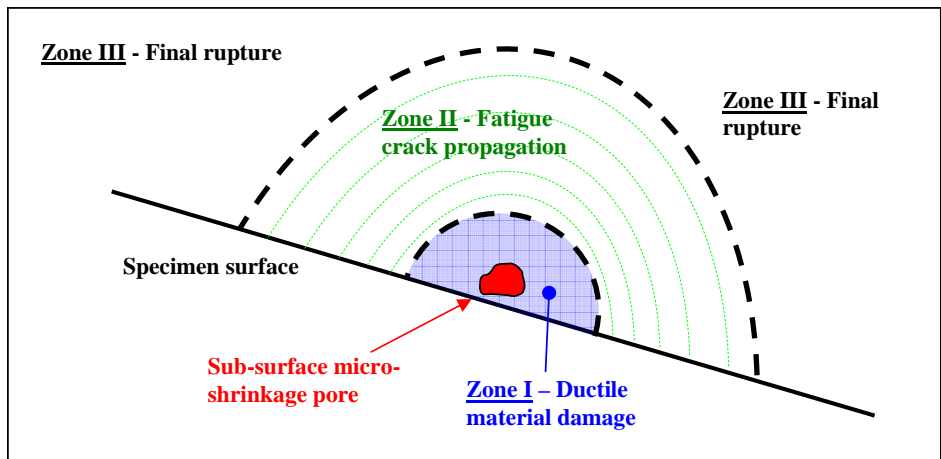


**Figure 8 – Schematic representation of the fatigue failure surface at R=0.95**

Therefore, at high mean stress, the high cycle fatigue mechanism is inherently associated with the material damage caused by the high stress levels (i.e. stress levels greater than the yield stress). A fatigue crack then initiates due to the local stress concentration created by the damage. This is different to the mechanism occurring at low mean stress where fatigue is controlled by micro-shrinkage pores.

This is a possible explanation of the different levels of scatter in the fatigue limits determined experimentally at low and high mean stress (see section 3). At high load ratio the variation in the size of the damaged zones is perhaps less, than the

variation in the size of the shrinkage pores, leading to lower scatter when the mean stress is high.

## 6 APPLICATION OF THE DANG VAN CRITERIA

The Dang Van criterion [5,6] is a multiaxial, high cycle, critical plane fatigue criterion, based on a multi-scale approach using the concept of elastic shakedown. That is, the fatigue process is considered both on the usual scale of the engineer (the macroscopic scale) and on the mesoscopic scale or the scale of individual grains of the material. The Lin-Taylor hypothesis is used in order to facilitate the passage from mesoscopic quantities (stress and strain) to macroscopic zones. The criteria can be summarized by the following statement: “Microscopic fatigue crack initiation does not occur if the material is shaken-down elastically at both the macroscopic and mesoscopic scales, or if the material adapts elastically at all scales”. This hypothesis has been verified at high mean stress for the material in question, at least at the macroscopic scale, by strain gauge measurements [1].

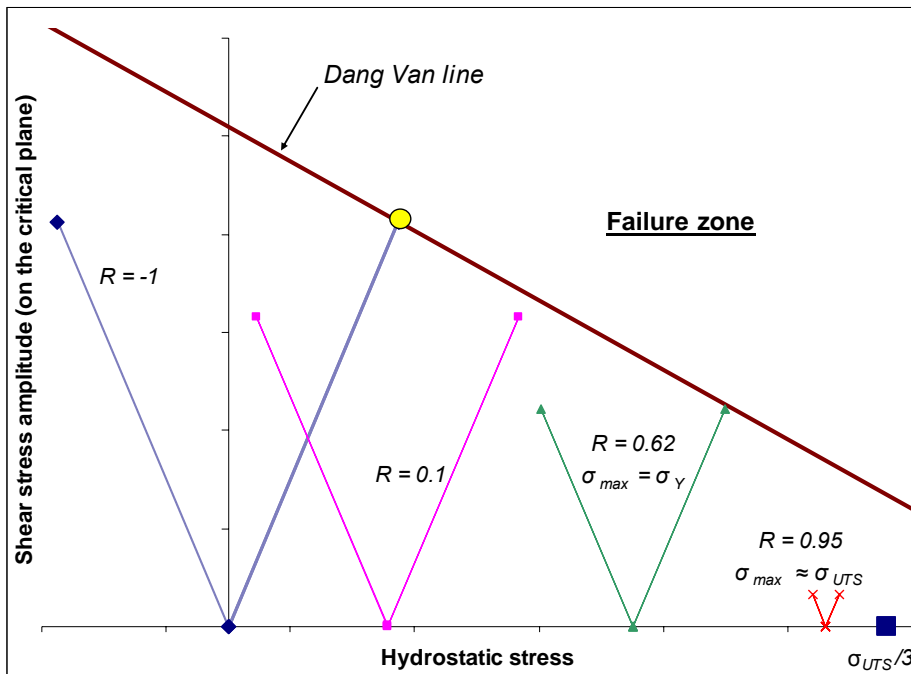


**Figure 9 – Application of the Dang Van criterion to the Al-Si cast aluminum alloy**

Mathematically the Dang Van criterion is represented by the equation 2:

$$\max_t \left\{ \max_n \left[ \|\underline{\tau}(n,t)\| + \alpha \sigma_H(t) \right] \right\} \leq \beta \quad (1)$$

Where  $\sigma_H(t)$  is the hydrostatic stress as a function of time and  $\underline{\tau}(n,t)$  is the mesoscopic shear stress (in the elastic shakedown state) on a material plane,

Deleted: 2

defined by its vector normal. The critical plane is determined via maximization over the cycle period and all possible material planes. The material parameters  $\alpha$  and  $\beta$  are determined via the push-pull fatigue limit and reversed torsional fatigue limit.

Figure 9 demonstrates the application of the criterion to the uniaxial fatigue limits discussed above. Note that as the torsional fatigue limit is unknown, the slope of the Dang Van line has been estimated using the available data. It can be seen that the criterion gives good predicts for the 3 fatigue limits in which the macroscopic stress state always remains elastic. For the case with very high mean stress ( $R = 0.95$ ), the criterion becomes non-conservative. This is a due to the change in mechanism discussed above, which is not taken into account in the criterion.

## 7 CONCLUSION AND FUTURE WORK

The motivation for this work is the “extreme” cyclic stress conditions found in diesel engine cylinder heads, where the stress amplitudes are very low, but the maximum stress can exceed the yield strength of the material.

From this work it can be concluded, for the Al-Si cast material investigated, that:

- A high cycle fatigue limit ( $2 \times 10^6$  cycles) exists for this material at very high load ratio ( $R=0.95$ ). In this cyclic stress state the maximum stress is very close to the ultimate tensile strength of the material.
- The experimental scatter observed in the fatigue limit (in terms of stress) is much lower when the mean stress is high.
- There is a change in fatigue crack initiation mechanism when the mean stress increases. It is believed that the transition occurs around the material yield strength.
- As discussed by other authors [3,4], at low mean stress (or R-ratio) fatigue crack initiation is controlled by the casting defects or micro-shrinkage pores.
- At high mean stress, the high cycle fatigue mechanism is inherently associated with material damage, primarily created in the first  $\frac{1}{4}$  cycle. This damage can be described as local rupture or decohesion of the material in the eutectic zones containing a large number of silicon particles (which are harder and more fragile than the phase  $\alpha$  aluminum dendrites). A fatigue crack consequently initiates (after cyclic loading at low stress amplitude) due to the local stress concentration created by the damage. The damage may or may not be associated with the casting defects.

It is envisioned that future work will include:

- Experimental investigation of the HCF fatigue mechanisms as a function of mean stress, in a biaxial cyclic stress state.
- Experimental investigation of the HCF fatigue mechanisms as a function of mean stress in other metallic materials. It is expected that material damage will continue to play a major roll at high R ratios.
- The development of a fatigue criterion capable of taking into account a change in mechanism. A model like that proposed by Monchiet [7] appears appropriate.

## 8 REFERENCES

1. **Bellett D, Morel F, (2007)** The effect of high hydrostatic stress in multiaxial high cycle fatigue, Proceedings: 8th International conference on multiaxial fatigue & fracture, Sheffield, England,
2. **Buffiere J.Y., Savelli S., Jouneau P.H., Maire E., Fougères R. (2001)** Experimental study of porosity and its relation to fatigue mechanisms of model Al-Si7-Mg0.3 cast AL alloy. Mater. Sci. Eng. A, Vol. 316, pp115-126, 2001
3. **Powell G.W. (1994).** The fractography of casting alloys. Mater. Char., vol. 33, pp 275–293.
4. **Couper M.J., Neeson A.E., Griffiths J.R. (1990).** Castings defects and the fatigue life of an aluminum casting alloy. Fatigue Fract. Eng. Mater. Struct., vol. 13, pp 213–227
5. **K. Dang Van, (1993),** Macro-Micro Approach in High-Cycle Multiaxial Fatigue, Advances in Multiaxial Fatigue, ASTM STP 1191, D.L. McDowell and R. Ellis, Eds., American Society for Testing and Materials, Philadelphia, 1993, pp. 120-130
6. **Constantinescu, A., Dang Van, K., Maitournam, M.H., (2003),** A unified approach for high and low cycle fatigue based on shakedown concepts. Fatigue Fract. Eng. Mater. Struct., Vol. 26 (6), pp. 561-568
7. **Monchiet V., Charkaluk E., Kondo D. (2008)** A micromechanical explanation of the mean stress effect in high cycle fatigue, Mech. Res. Commun.

## ACKNOWLEDGMENTS

This work is being performed, in a partnership including PSA Peugeot-Citroën.